



## The Arctic picoeukaryote *Micromonas pusilla* benefits from Ocean Acidification under constant and dynamic light

5 Emily White<sup>1</sup>, Clara J.M Hoppe<sup>1</sup>, Björn Rost<sup>1,2</sup>

<sup>1</sup>Alfred-Wegener-Institut – Helmholtz-Zentrum für Polar- und Meeresforschung, Bremerhaven, 27570, Germany

<sup>2</sup>Universität Bremen, FB2, Leobener Strasse, 28359 Bremen, Germany

10 Correspondence to: Emily White (ewhite14@msn.com)

**Abstract.** Compared to the rest of the globe, the Arctic Ocean is affected disproportionately by climate change. Despite  
15 these fast environmental changes, we currently know little about the effects of ocean acidification (OA) on marine key  
species in this area. Moreover, the existing studies typically test the effects of OA under constant, hence artificial light fields.  
In this study, the abundant Arctic picoeukaryote *Micromonas pusilla* was acclimated to current (400  $\mu\text{atm}$ ) and future (1000  
 $\mu\text{atm}$ )  $p\text{CO}_2$  levels under a constant as well as dynamic light, simulating natural light fields as experienced in the upper  
mixed layer. To describe and understand the responses to these drivers, growth, particulate organic carbon (POC)  
20 production, elemental composition, photophysiology and reactive oxygen species (ROS) production were analysed. *M.*  
*pusilla* was able to benefit from OA on various scales, ranging from an increase in growth rates to enhanced photosynthetic  
capacity, irrespective of the light regime. These beneficial effects were, however, not reflected in the POC production rates,  
which can be explained by energy partitioning towards cell division rather than biomass build-up. In the dynamic light  
regime, *M. pusilla* was able to optimise its photophysiology for effective light usage during both low and high light periods.  
25 This effective photoacclimation, which was achieved by modifications to photosystem II (PSII), imposed high metabolic  
costs leading to a reduction in growth and POC production rates when compared to constant light. There were no significant  
interactions observed between dynamic light and OA, indicating that *M. pusilla* was able maintain effective  
photoacclimation without increased photoinactivation under high  $p\text{CO}_2$ . Based on these findings, physiologically plastic *M.*  
*pusilla* may exhibit a robust positive response to future Arctic Ocean conditions.



30

## 1 Introduction

Alterations to the ecosystem caused by climate change are far more pronounced in the Arctic than in the rest of the world (Pörtner et al., 2014). The increase in  $p\text{CO}_2$  and concomitant decrease in seawater pH, for instance, is particularly fast in the Arctic Ocean, which is mainly due to the higher solubility of  $\text{CO}_2$  at low water temperatures (Bates and Mathis, 2009). Many studies have investigated the effects of ocean acidification (OA) on phytoplankton and have observed species-specific responses (Lohbeck et al., 2012; Riebesell and Tortell, 2011; Rost et al., 2008). The negative effects of OA are thought to result from disturbed ion homeostasis under decreasing pH, while positive responses seem to be driven by the physiological mechanisms of inorganic carbon uptake (Bach et al., 2013; Rokitta et al., 2012). Photosynthesis requires  $\text{CO}_2$  as a substrate for the carbon-fixing enzyme RubisCO, which is yet characterized by a poor substrate affinity. To avoid  $\text{CO}_2$  limitation arising from this, especially larger phytoplankton typically depend on carbon-concentrating mechanisms (CCMs). These CCMs involve the transport of  $\text{CO}_2$  and/or  $\text{HCO}_3^-$  into the cell, the prevention of leakage out of the cell, as well as the expression of carbonic anhydrase, an enzyme accelerating the interconversion between  $\text{CO}_2$  and  $\text{HCO}_3^-$  (Reinfelder, 2011). As CCMs are energetically expensive, a potential downregulation under OA may be beneficial for phytoplankton (Hopkinson et al., 2011).

Also the rates of warming are two to three times faster than the global average (Trenberth et al., 2007), a phenomenon known as Arctic amplification (Miller et al., 2010). Warming causes changes to mixing regimes in the surface ocean (Houghton et al., 2001), probably leading to a shoaling of the mixed layer due to increased thermal stratification and freshening caused by sea-ice melting (Steinacher et al., 2010). From model predictions, the Arctic Ocean will become nearly ice-free during the summer more and more frequently (Pachauri et al., 2014). With a decrease in sea-ice cover the primary productivity in the Arctic is expected to increase due to a longer growing season for phytoplankton (Arrigo et al., 2008). At the same time, however, annual productivity may get increasingly limited by the low nutrient supply in the Arctic Ocean, which may decrease even further due to reduced upwelling (Tremblay et al., 2015; Wassmann and Reigstad, 2011). These environmental changes in the Arctic have already led to changes in community structure and are expected to cause more dramatic regime shifts in the future (e.g. Nöthig et al., 2015; Li et al., 2009).

Next to climate driven changes, phytoplankton growing in the turbulent upper mixed layer must generally acclimate changes to the dynamics of light availability. Due to the low light periods in such dynamic light fields, phytoplankton on the one hand need to increase the light harvesting efficiency, e.g. by increasing the photosynthetic pigments like chlorophyll *a* (Chl *a*) (Palmer et al., 2013). In the high light periods, on the other hand, photoprotective mechanisms need to be activated to prevent photodamage to cells (Ragni et al., 2008). There are species-specific differences in the responses to differing light regimes, which can include changes in the amount of photoprotective pigments, different photorepair mechanisms and modifications to the number of reaction centres in PSII (Ragni et al., 2008). Such acclimatory responses may be particularly important in the Arctic shelf seas, where high organic matter loading lead to particularly high light attenuation with depth (Granskog et al., 2012).

In the world's oceans, the picoplanktonic size fraction (2-3  $\mu\text{m}$ ) dominates primary productivity (Worden et al., 2015) and *Micromonas*-like picoeukaryotes are highly abundant in the Arctic region already today (Lovejoy et al., 2007). *Micromonas* has been described as a shade-adapted species that can persist in Arctic winter darkness (Marquardt et al., 2016) with the help of mixotrophy (McKie-Krisberg and Sanders, 2014). Such low-light adapted organisms are thought to show a lack of plasticity with regard to Chl *a* quota and photoacclimation (Talmy et al., 2013). Smaller phytoplankton are furthermore expected to particularly benefit from reduced nutrients under enhanced stratification due to their high surface : volume ratio, which allows them to take up nutrients more efficiently (Brussaard et al., 2013). For the same reasons, picoeukaryotes may benefit from elevated  $p\text{CO}_2$  levels due to increased  $\text{CO}_2$  diffusion into the cell. Concurrently, it has been



shown that smaller phytoplankton will thrive under future OA conditions in different experiments (Brussaard et al., 2013; Engel et al., 2008; Hoppe et al., 2017; Hoppe et al., 2018; Maat et al., 2014; Meakin and Wyman, 2011; Schulz et al., 2017) and are regarded as potential ‘winners’ of climate change (e.g. Hoppe et al., 2018; Li et al., 2009; Schulz et al., 2017).

Despite their prevalence in all marine habitats, previous studies on OA effects have mostly disregarded the effect of natural light variability. In previous studies, however, fluctuating light has been reported to affect phytoplankton photosynthesis and growth (Falkowski, 1980; Huisman, 1999; Köhler et al., 2018; Litchman, 2000; Litchman et al., 2004). Interactive effects between dynamic light regimes and OA have been observed in the coccolithophore *Gephyrocapsa oceanica*, causing decreased productivity (Jin et al., 2013). Hoppe and co-workers (2015) reported that the Antarctic diatom *Chaetoceros debilis* benefitted from OA under static irradiance, while a dynamic light regime reversed this positive response. This was attributed to the fact that OA-dependent downregulation of the CCM can expose cells to oxidative stress during high light peaks under dynamic light (Hoppe et al., 2015). Oxidative stress occurs when the production of reactive oxygen species (ROS) exceeds the defensive mechanisms for ROS reduction, leading to accumulation in the cells (Apel and Hirt, 2004). In this study, the response of *M. pusilla* to OA was investigated under constant and dynamic light in order to determine if there was an interactive effect of the two environmental factors. A particular focus was laid on the physiological mechanisms that determined the observed overall responses.

## 2 Materials and Methods

### 2.1 Experimental set up

Monoclonal cultures of the picoeukaryote *M. pusilla* (isolated in 2014 by Klara Wolf in Kongsfjorden, Svalbard, 79°N) were grown in 1 L glass bottles in semi-continuous dilute batch cultures (max. 158000 cells ml<sup>-1</sup>; diluted every 3-5 days). The temperature remained stable at 2.6 ± 0.2°C. The media was composed of Arctic seawater (from AWI-Hausgarten, 78°N, collected during an RV *Merian* cruise in 2013) filtered through a 0.2 µm membrane filter capsule (Satorius stedium Biotech, Sartobran 300) and enriched with vitamins and trace metals in accordance to the F/2 protocol (Guillard and Ryther, 1962), as well as with macronutrients in Redfield proportions (containing 100 µmol L<sup>-1</sup> of nitrate and silicate, and 6.2 µmol L<sup>-1</sup> phosphate).

Both the constant and the dynamic light regime consisted of a 20:4h light:dark cycle with an average light intensity of 83 ± 5 µmol photons m<sup>2</sup> s<sup>-1</sup>. The dynamic light regime varying between 0 and 590 µmol photons m<sup>2</sup> s<sup>-1</sup> (Fig. 1). These light levels were calculated based on conditions typically observed on the Arctic Kongsfjorden (Svalbard, 79°N) in late spring, using maximum surface irradiance of 905 µmol photons m<sup>2</sup> s<sup>-1</sup>, a mixed-layer depth of 20 m, an extinction coefficient of 0.35 m<sup>-1</sup> (C. Hoppe, unpublished results) and a vertical mixing rate of 0.011 m s<sup>-1</sup> (Denman and Gargett, 1983). Light was supplied through LED lamps (ECONLUX, Solar Stinger Sunstrip, ECONLUX), and the dynamic light regime was regulated using a daylight controller (LED light scaping control, LiWeBe). In both setups, the light levels were monitored using a ULM-500 universal light meter with a 4π sensor (Effeltrich) and light intensity was adjusted with neutral density screens.

The CO<sub>2</sub> partial pressures (*p*CO<sub>2</sub>) were achieved through aeration of the incubation bottles with two different *p*CO<sub>2</sub> levels (400 and 1000 µatm) for at least 12 h prior to inoculation. The gas mixtures were created using a gas flow controller (CGM 2000 MCZ Umwelttechnik), which mixed pure CO<sub>2</sub> with CO<sub>2</sub>-free air to the desired *p*CO<sub>2</sub> level. The *p*CO<sub>2</sub> levels were monitored using a non-dispersive infrared analyser (LI6252; Li Cor Biosciences). The humidified gas mixtures were bubbled through a glass frit and supplied via a sterile 0.2 µm PTFE filter (Midistart 2000, Satorius stedium). Cultures were acclimated to the respective *p*CO<sub>2</sub> levels for at least 5 generations prior to the experiment. To minimize shifts in carbonate chemistry due to biomass production, cell densities were kept low between 5000 and 158000 cells ml<sup>-1</sup>.



## 2.2 Carbonate chemistry

120 Seawater pH was determined potentiometrically, using a two-point calibrated glass reference electrode (IOline, Schott  
Instruments) and pH meter (826 pH mobile, Metrohm), and reported on the NBS scale for incubation temperatures. The  
samples for dissolved inorganic carbon ( $C_T$ ) measurements were gently filtered through a sterile 0.2  $\mu\text{m}$  nalgene syringe  
filter (Nalgene, Thermo scientific) and stored in in the dark at 2°C in 5 ml borosilicate bottles. The sample was subsequently  
125 analysed colorimetrically in duplicate using an auto analyser (Seal Analytical; Stoll et al., 2001) with a reproducibility of  $\pm 8$   
 $\mu\text{mol kg}^{-1}$  (Table 1). A certified reference standard material (CRM) was used to correct for measurement errors (Dickson et  
al., 2007). The final average  $C_T$  values were  $2131 \pm 17 \mu\text{mol kg}^{-1}$  at ambient  $p\text{CO}_2$  levels and  $2195 \pm 12 \mu\text{mol kg}^{-1}$  under  
high  $p\text{CO}_2$  (Table 1). The total alkalinity ( $A_T$ ) samples were gently filtered through pre-combusted 25 mm GF/F filters (glass  
microfiber filter, Whatman, GE Healthcare Life sciences) and stored in 125 ml dark borosilicate bottles at 2°C. Standards  
and samples were equilibrated to room temperature prior to potentiometric titrations (Brewer et al., 1986) of two 25 ml  
130 subsamples with an auto analyser (Titroline alpha plus, SCHOTT instruments). An internal standard was applied to correct  
for systematic errors based on measurements of CRMs, and the data was processed using TitrSoft 2.71 software. The  
corrected final  $A_T$  values ranged between  $2194 \pm 8 \mu\text{mol kg}^{-1}$  and  $2216 \pm 6 \mu\text{mol kg}^{-1}$  (Table 1). The full carbonate system  
was calculated with a salinity of 32.2 and a temperature of 2°C using the pH and  $A_T$  data with the  $\text{CO}_2\text{SYS}$  program (Pierrot et  
al., 2006). The calculations used constants of Mehrbach et al., (1973) with a refit by Dickson and Millero (1987) and a ( $B_T$ )  
135 value according to Uppström, (1974). The carbonate system remained stable for the duration of the experiment, as  $C_T$   
drawdown was  $<2\%$  and the average daily pH values were  $8.13 \pm 0.06$  for ambient conditions and  $7.81 \pm 0.03$  for high  
 $p\text{CO}_2$  levels (Table 1).

## 2.3 Growth and cellular composition

140 Cell densities of *M. pusilla* were quantified using a flow cytometer (FCM; BD Biosciences, Accuri C6). Samples were  
analysed using live cells, where 490  $\mu\text{l}$  of sample was added to 10  $\mu\text{l}$  of 1  $\mu\text{m}$  microspheres fluorescent beads solution  
(Polysciences Inc, Fluoresbrite YG), which acted as an internal standard. Cells were identified and counted using the FL3  
and FL4 channels as well as forward scatter for 2 minutes on slow speed with a maximum of 50,000 events. Specific growth  
145 rate constants ( $\mu$ ) were calculated from exponential fits of cell numbers over time for each replicate bottle. Samples were  
measured daily within a 1 h timeframe for consistency.

Samples for particulate organic carbon (POC) and nitrogen (PON) were gently filtered onto pre-combusted 25 mm  
GF/F filters. Before analysis, 200  $\mu\text{l}$  of hydrochloric acid (HCl, 0.2  $\mu\text{mol L}^{-1}$ ) was added to each filter and the samples were  
dried at 60°C for at least 12 h to remove any inorganic carbon. The samples were analysed using an elemental analyser (Euro  
150 EA 3000, HEKAtech). The POC and PON data was corrected by subtracting blank measurements, and values were  
normalised using the specific cell density and volume filtered to yield cell quotas. Subsequently, production rates were  
calculated by multiplying the quota with the division rate constant  $k$  ( $k = \mu/\ln(2)$ ) of the respective incubation.

Samples for Chl *a* quota were obtained by gentle filtration onto 25 mm GF/F filters and immediately stored at -  
20°C until analysis. For chlorophyll extraction, 8 ml of 90% acetone was added to the filters and subsequently stored at 4°C  
155 for at least 2 h. After centrifugation (4500 rpm for 5 min, Sigma 4K10), samples were measured on a fluorometer (TD-700  
Fluorometer, Turner designs) before and after acidification with HCl (1  $\mu\text{mol L}^{-1}$ ). Chl *a* concentrations ( $\mu\text{g L}^{-1}$ ) were  
calculated as in Knap et al., (1996).



160

## 2.4 Physiological responses

165 Photophysiological parameters were measured using a fast repetition rate fluorometer (FRRf; FastOcean sensor, Chelsea technologies) in combination with a FastAct system (Chelsea technologies). The fluorometer's light emitting diodes (LEDs) were set to an emission wavelength of 450 nm. A saturation phase of 100 flashlets on a pitch of 2  $\mu$ s was used, with a relaxation phase comprising of 40 flashlets and a pitch of 50  $\mu$ s. Prior to measurements, samples were dark acclimated for 15 min and measurements were conducted in a temperature-controlled chamber at 3 °C. The maximum ( $F_m$ ,  $F'_m$ ) and minimum ( $F_0$ ,  $F'_0$ ) chlorophyll fluorescence in the dark and light were estimated according to iterative algorithms for induction (Kolber et al., 1998) and relaxation phase (Oxborough et al., 2012). The PSII quantum yield efficiency was estimated as  $F_v/F_m$  using the following equation:

$$F_v/F_m = (F_m - F_0)/F_m \quad (1)$$

175 Additional parameters were measured after dark acclimation, including the absorption cross-section size of PSII ( $\sigma_{\text{PSII}}$ ; [ $\text{\AA}^2 \cdot \text{q}^{-1}$ ]), the connectivity of PSII ( $\rho$ ) and the PSII re-opening rate ( $\tau$ ; [ms]), according to Kolber et al., (1998).  $F'_0$  was estimated after Oxborough and Baker (1997) as

$$F'_0 = F_0 \frac{F_v}{F_m} + \frac{F_0}{F'_m} \quad (2)$$

Thereafter, the coefficient of photochemical quenching  $q_L$  was calculated after Kramer et al., (2004) as

$$q_L = (F'_m - F') / (F'_m - F'_0) * (F'_0 / F') \quad (3)$$

180 The electron transport rates through PSII (ETR; [ $\text{mol e}^- (\text{mol RCII})^{-1} \text{s}^{-1}$ ]) were calculated after Xu et al., (2017) using the following equation:

$$ETR = \sigma_{\text{PSII}} \times q_L \times PAR \quad (4)$$

where  $\sigma_{\text{PSII}}$  is the absorption cross-section size of PSII,  $q_L$  is the coefficient of photochemical quenching, and PAR is the photosynthetically active radiation. Photosynthesis-irradiance (PI) curves were estimated at eight irradiances between 0 and 589  $\mu\text{mol photons m}^{-2} \text{s}^{-1}$ . According to the model by Webb et al., (1974), the light harvesting efficiency ( $\alpha$ ; [ $\text{mol e}^- \text{m}^2 (\text{mol RCII})^{-1} (\text{mol photons})^{-1}$ ]) and the maximum relative electron transport rate ( $ETR_{\text{max}}$ ; [ $\text{mol e}^- (\text{mol RCII})^{-1} \text{s}^{-1}$ ]) were estimated using the following equation:

$$ETR = ETR_{\text{max}} \left[ 1 - e^{\left( \frac{-\alpha I}{ETR_{\text{max}}} \right)} \right] \quad (5)$$

The light saturation index ( $I_k$ ; [ $\mu\text{mol photons m}^{-2} \text{s}^{-1}$ ]) was calculated as  $ETR_{\text{max}} / \alpha$ .

190 At the maximum light level of 506  $\mu\text{mol photons m}^{-2} \text{s}^{-1}$ , non-photochemical quenching (NPQ) was calculated as  $Y(\text{NPQ})$  using calculations as described in Klughammer & Schreiber (2008):

$$Y(\text{NPQ}) = \frac{F}{F'_m} - \frac{F}{F_m} \quad (6)$$

195 Measurements of oxidative stress for both  $\bullet\text{O}_2^-$  free radicals and  $\text{H}_2\text{O}_2$  were assessed using the FCM with the fluorochromes dihydroethidium (HE; Sigma Aldrich, D7008) and dihydrorhodamine 123 (DHR123; Sigma Aldrich, D1054), respectively. Methods were adapted from Prado et al., (2012), with final dye concentrations adjusted to 158.5  $\mu\text{M}$  for the fluorochrome HE and 28.87 mM for DHR123, and an optimized incubation time of 30 min in the dark at 2 °C. Gated FL1 (505 - 550 nm) and FL3 (600 - 645 nm) detection channels were used to analyse the relative concentration of  $\bullet\text{O}_2^-$  free radicals and  $\text{H}_2\text{O}_2$ , respectively. The oxidative stress measurements were corrected using blank measurements and normalised to cell size using the forward scatter.

200 The oxidative stress measurements were taken at two specific time points on the last day of incubation, whereas the photophysiological measurements were taken solely at time point 2 (Fig. 1). The midday measurements, referred to as time



point 1, were conducted at the highest light intensity ( $590 \mu\text{mol photons m}^{-2} \text{s}^{-1}$ ) in the dynamic light cycle, and at the same time under the average light intensity ( $83 \mu\text{mol photons m}^{-2} \text{s}^{-1}$ ) in the constant light cycle. The evening measurements, referred to as time point 2, were conducted at the start of the dark period ( $0 \mu\text{mol photons m}^{-2} \text{s}^{-1}$ ) in both the constant and dynamic light cycle.

205

### 3 Results

#### 210 3.1 Growth and cellular composition

In this study, the growth rates of *M. pusilla* were affected by both, light regime and  $p\text{CO}_2$  level (Fig. 2). Growth was reduced by at least 50 % in dynamic versus constant light, irrespective of  $p\text{CO}_2$  level (ANOVA,  $F=562.1$ ,  $p<0.0001$ ). In addition, growth rates significantly increased ( $>4$  %) under elevated  $p\text{CO}_2$  levels in both light regimes (ANOVA,  $F=17.1$ ,  $p=0.0014$ ).  
215 The POC and PON quotas were not altered by changes in light regime or  $p\text{CO}_2$  levels (Table 2). The POC production rates were significantly higher in constant versus dynamic light (ANOVA,  $F=72.6$ ,  $p<0.0001$ ), irrespective of the  $p\text{CO}_2$  level applied (Fig. 2). The C:N ratio was not significantly affected by the applied treatments (Fig. 2, Table 2). While Chl *a* quotas decreased significantly under elevated  $p\text{CO}_2$  levels (ANOVA,  $F=26.4$ ,  $p=0.0002$ ), there was no significant response to the light treatments applied (Fig. 2). The applied treatments did not have a significant effect on the C:Chl *a* ratio (Table 2). For  
220 all these parameters, no significant interactive effects between the applied light and  $p\text{CO}_2$  conditions could be detected.

#### 3.2 Photophysiological measurements

The FRRf measurements yielded a number of physiological parameters, most of which were significantly affected by the  
225 different light and/or  $p\text{CO}_2$  treatments applied (Table 3). The PSII quantum yield efficiency ( $F_v/F_m$ ) under dynamic light was significantly higher compared to the constant light treatment (ANOVA,  $F=88.5$ ,  $p<0.0001$ ; Table 3). Even though to a lesser extent, high  $p\text{CO}_2$  levels also significantly increased the  $F_v/F_m$  (ANOVA,  $F=4.8$ ,  $p=0.0480$ ; Table 3). The connectivity of PSII ( $\rho$ ) was higher under dynamic versus constant light (ANOVA,  $F=17.6$ ,  $p=0.0011$ ), while there was no significant effect of  $p\text{CO}_2$  (Table 3). Similarly, the absorption cross-section of PSII photochemistry ( $\sigma_{\text{PSII}}$ ) was significantly higher in dynamic  
230 compared to constant light (ANOVA,  $F=77.0$ ,  $p<0.0001$ ), irrespective of the applied  $p\text{CO}_2$  level (Table 3). In addition, there was significantly less NPQ under dynamic compared to constant light (ANOVA,  $F=212.9$ ,  $p<0.0001$ ), with values being lower under dynamic light (Table 3). However, there was no significant  $p\text{CO}_2$  response in NPQ ( $p>0.05$ ). Under dynamic light, the PSII re-opening rate ( $\tau$ ) was significantly and  $>5$  % lower when compared to constant light (ANOVA,  $F=18.6$ ,  $p=0.0008$ ), while the  $\tau$  did not display a significant response to  $p\text{CO}_2$  (Table 3).

235 The model by Webb et al., (1974) was used to estimate P-I parameters from the FRRf data. The light saturation index ( $I_k$ ) and maximum photosynthetic rate ( $\text{ETR}_{\text{max}}$ ) increased both significantly by  $>10$  % under elevated  $p\text{CO}_2$  levels (ANOVA,  $F=11.8$ ,  $p=0.0047$  for  $I_k$  and  $F=6.8$ ,  $p=0.0214$  for  $\text{ETR}_{\text{max}}$ ; Table 3). While there was no significant response of  $I_k$  to the two light treatments,  $\text{ETR}_{\text{max}}$  was significantly higher under dynamic light compared to constant light (ANOVA,  $F=41.2$ ,  $p<0.0001$ , Table 3). The light harvesting efficiency ( $\alpha$ ) was significantly reduced by high  $p\text{CO}_2$  versus ambient  
240  $p\text{CO}_2$  levels (ANOVA,  $F=9.6$ ,  $p=0.0084$ ).  $\alpha$  was also significantly higher under dynamic light compared to constant light (ANOVA,  $F=36.0$ ,  $p<0.0001$ , Table 3).



### 3.3 Oxidative stress measurements

245

The relative concentrations of  $\bullet\text{O}_2^-$  free radicals and  $\text{H}_2\text{O}_2$  were used as an indication of oxidative stress under the applied treatments. At time point 1 (midday), the production of  $\bullet\text{O}_2^-$  free radicals was not significantly changed in response to  $p\text{CO}_2$  levels or light regimes ( $p>0.05$ ; Fig. 3). However, there was a significant increase in  $\text{H}_2\text{O}_2$  production in high  $p\text{CO}_2$  versus ambient  $p\text{CO}_2$  conditions (ANOVA,  $F=4.8$ ,  $p=0.0488$ ), irrespective of the light treatment applied (Fig. 3). The applied

250

treatments did not have a significant effect on the oxidative stress measurements at time point 2 (Fig. S1, in the Supplement).

## 4 Discussion

### 4.1 Effective acclimation towards dynamic light imposes high metabolic costs

255

In their natural environment, phytoplankton need to cope with varying light in the upper mixed layer (MacIntyre et al., 2000). Next to variation in insolation, the light fields are critically dependent on the mixed layer depth, the light attenuation and the vertical mixing rate. In laboratory experiments, however, they are often exposed to an artificially constant light (Köhler et al., 2018). Simulating a typical light regime in an Arctic Fjord, we could show that *M. pusilla* can photoacclimate to natural variations in light availability without showing signs of high-light stress. This is supported by significantly higher PSII quantum yield efficiency ( $F_v/F_m$ ) under dynamic light (Table 3), which is commonly used as a health indicator of photosynthetic organisms, indicating successful photoacclimation to varying light intensities (Van Leeuwe and Stefels, 2007).

260

To achieve this photoacclimation, *M. pusilla* can apparently adjust its PSII physiology to balance photoprotection during high light periods with sufficient absorption during low-light periods of the dynamic light field. More specifically, there were a number of changes to PSII, including a significant increase in the cross-section size of the antenna in PSII ( $\sigma_{\text{PSII}}$ ), an increase in the connectivity between PSIIs ( $\rho$ ) and quicker PSII re-opening rates ( $\tau$ ; Table 3). An increase in  $\sigma_{\text{PSII}}$  acts to increase the absorption of light (Suggett et al., 2007), which would have been beneficial within the low-light periods of the dynamic light cycle (Schuback et al., 2017), and which is supported by a significant increase in the light harvesting efficiency under low-light ( $\alpha$ ; Table 3). The observed increase in  $\rho$  under dynamic light allows higher flexibility to capture electrons during low light phases while at the same time allowing excess excitation energy to be redistributed among PSII centres during high light phases. This increases energy capture efficiency while protecting the PSII centres from damage through migration of excitation energy between different PSIIs also termed the ‘Lake model’ (Blankenship, 2014; Trimborn et al., 2014), highlighting that *M. pusilla* has high potential for photoprotection. Additionally, the higher  $\tau$  under dynamic versus constant light indicates more efficient drainage of electrons down-stream of PSII (Kolber et al., 1998). A faster PSII re-opening rate can also compensate for deactivation of functional PSII reaction centres during the high light periods of the dynamic light field (Behrenfeld et al., 1998). The significantly lower NPQ in combination with higher  $\text{ETR}_{\text{max}}$  under dynamic versus constant light reflects photoacclimation to a higher light intensity under dynamic light, allowing effective utilization of high excitation energy without initiating high-light stress (Ragni et al., 2008). Consequently, *M. pusilla* exhibits the physiological plasticity needed to prevent photodamage, which otherwise can disturb the balance between production and scavenging of reactive oxygen species (ROS), causing oxidative stress and accumulation of ROS (Apel and Hirt, 2004). Indeed, dynamic light did not cause increased ROS production in response to the dynamic light field (Fig. 3). Overall, the PSII physiology of *M. pusilla* was effectively acclimated to naturally varying light, displaying photoprotection strategies during high-light phases and upregulated light harvesting during low-light phases.

265

270

275

280



285 The described photoacclimation strategies appear to come at a cost, namely lowered energy transfer efficiency to  
biomass build-up, which is supported by significantly lower growth rates and POC production, despite an increase in  $F_v/F_m$   
and  $ETR_{max}$  under dynamic compared to constant light (Fig. 2, Table 3). Our findings agree with previous studies, which also  
290 found lowered growth under a dynamic light regime (Hoppe et al., 2015; Jin et al., 2013; Mills et al., 2010; Shatwell et al.,  
2012, Su et al., 2012; Wagner et al., 2006). Changes in light regime strongly influence relationships between  
photochemistry, carbon fixation and downstream metabolic processes, optimizing light harvesting to sustain growth  
(Behrenfeld et al., 2008). In view of this, the significant changes to PSII physiology (Table 3) suggest that resources were  
channelled towards light harvesting rather than protein synthesis and biomass build-up (Talmy et al., 2013). Therefore, it can  
be concluded that the lower growth rates in dynamic light were caused by the high metabolic costs associated with  
photoacclimation to the varying light intensities and not due to photoinhibition. Thus, our results stand in contrast to  
295 previous evidence that suggests *Micromonas* to be a shade adapted genus (Lovejoy et al., 2007), as such low-light adapted  
species are expected to possess limited plasticity in photoacclimative capabilities (Talmy et al., 2013).

#### 4.2 Picoeukaryotes benefit from ocean acidification irrespective of the light regime

300 The low Arctic temperatures enhance  $CO_2$  solubility, and therefore OA, of which photosynthetic organisms may benefit due  
to increased  $CO_2$  availability for photosynthesis (AMAP, 2018). This seems true for picoeukaryotes, as in this study *M.*  
*pusilla* showed increased growth rates and photophysiological efficiency under elevated  $pCO_2$  (Table 2; Fig. 2). These  
results are in line with various studies that have reported picoeukaryotes to benefit from increasing  $pCO_2$  (Brussaard et al.,  
2013; Hoppe et al., 2018; Meakin and Wyman, 2011; Newbold et al., 2012; Schaum et al., 2013, Schulz et al., 2017). In the  
305 current study, however, there was no observed increase in POC production (Fig. 2) under higher  $pCO_2$  levels, which could  
be expected assuming lowered costs due to CCM down-regulation (Iglesias-Rodriguez et al., 1998; Rost et al., 2008). The  
observed increase in growth rates nonetheless indicates beneficial OA effects, potentially due to re-allocation of energy  
liberated by eased carbon acquisition. Alternatively, the large surface : volume ratio of *M. pusilla* (cell size of 2-3  $\mu m$ ) may  
generally lower the need for an active CCM, allowing cells to dependent more strongly on diffusive  $CO_2$  uptake (Falkowski  
and Raven, 2013). As the latter is directly linked to the  $pCO_2$  level, it could likewise explain the higher growth rates  
310 observed under elevated  $pCO_2$ . In any case, the growth strategy of the investigated strain involves energy allocation into cell  
division rather than biomass build-up. Whether picoeukaryotes such as *M. pusilla* benefit from OA due to increased diffusive  
 $CO_2$  uptake or lowered CCM costs remains to be tested.

To further explain the increase in growth rate under elevated  $pCO_2$ , it is essential to look into the upstream  
315 physiological parameters. There was a significant increase in the  $ETR_{max}$  under OA (Table 3), which indicates an increase in  
photosynthetic capacity. Previous studies on picoeukaryotes have reported variable results with studies displaying no change  
or an increase in  $ETR_{max}$  in response to OA (Brading et al., 2011; Fu et al., 2007; Kim et al., 2013). In this study,  $I_k$  increased  
in concert with  $ETR_{max}$  with increasing  $pCO_2$  (Table 3). This ' $I_k$ -dependent behaviour' is known as acclimation to higher  
light levels in order to optimize balanced growth (Behrenfeld et al., 2008). In the current case, the increase in  $I_k$  under OA  
320 could indicate that eased carbon acquisition shifted the balance of energy acquisition and its sinks towards saturation at  
higher irradiances, which fits to the reduced Chl *a* quota under these conditions (Fig. 2). At the same time, also the light  
harvesting efficiency at low light ( $\alpha$ ; please note this unit is per photosystem) decreased in response to OA (Table 3). Such  
' $I_k$ -independent behaviour' is influenced by changed in the relative contribution of different sinks of photosynthetic energy,  
namely carbon fixation, direct use and ATP generation via cyclic electron transport and other mechanisms (Behrenfeld et al.,  
325 2008). Both photoacclimative strategies mimicked acclimation to high-light in response to increasing  $pCO_2$ , which may be a  
general OA response of phytoplankton (e.g. Hoppe et al. 2015, Rokitta & Rost 2012). At the same time, reduced Chl *a* quota  
indicate that such efficient photosystems decreased the need to invest into the total number of them. This potentially



330 balances the reductive pressure on the entire cell, as we did not observe any high-light stress, even during peaks (Fig. 3).  
Although there was a significant increase in H<sub>2</sub>O<sub>2</sub> concentration under OA relative to ambient pCO<sub>2</sub> levels, no change in  
•O<sub>2</sub><sup>-</sup> concentration was observed (Fig. 3). Thus, even if ROS production was enhanced under OA, efficient detoxification  
mechanisms (e.g. reduction of •O<sub>2</sub><sup>-</sup> to H<sub>2</sub>O<sub>2</sub>, (Asada, 1999)) seem to be in place. Additionally, changes to H<sub>2</sub>O<sub>2</sub> concentration  
have been linked to changes in growth metabolism under non-stressful conditions (Kim et al., 2004), which would fit to the  
'I<sub>k</sub>-independent behaviour' observed here, and suggests that sufficient sinks for the enhanced flow of photosynthetic energy  
were present. Thus, there is ample evidence that, despite no effect on biomass build-up, elevated pCO<sub>2</sub> facilitated carbon  
335 acquisition, led to faster and cheaper photosynthetic energy generation, and higher rates of cell division.

The described changes in photoacclimation were not partnered with a significant increase in POC production, despite  
an increase in growth rate (Fig. 2). These findings contrast with Hoppe et al., (2018), who reported that POC production  
rates were generally increased under OA. In this earlier study, however, the Chl *a* quota of *M. pusilla* remained relatively  
constant over a large range of pCO<sub>2</sub> levels at two temperatures, so that OA effects on the ratio between energy allocated into  
340 photosynthesis (i.e. Chl *a*) and biomass build-up (i.e. POC) in both studies actually agree. Furthermore, if only the pCO<sub>2</sub>  
levels investigated in the current study are considered from Hoppe et al., (2018), varying OA responses (i.e. decreasing vs.  
increasing for POC production, and constant vs. increasing for Chl *a* quota) were observed depending on the applied  
temperatures. This hints towards the well-known fact that even small changes in the environmental conditions can greatly  
modulate OA-responses of phytoplankton (Riebesell and Gattuso, 2015; Rost et al., 2008). In fact, differences between the  
345 two studies could also be caused by differences in the average irradiances (approx. 80 vs. 150 μmol photons m<sup>-2</sup> s<sup>-1</sup>). Despite  
these differences one should note, however, that high growth rates were obtained under the various OA treatments. As  
growth rate is the best available fitness indicator for single strain studies (Schaum and Collins, 2014), our findings is  
indicative for improved fitness of *M. pusilla* under OA.

#### 350 4.3 *M. pusilla* response does not indicate interactions between light regime and pCO<sub>2</sub>

The interaction between light field and OA has been investigated for the coccolithophore *Gephyrocapsa oceanica* (Jin et al.,  
2013) and the Antarctic diatom *Chaetoceros debilis* (Hoppe et al., 2015). In both studies, the species' increased their  
photochemical performance in response to elevated pCO<sub>2</sub> under constant light. Dynamic light fields reversed the positive  
355 effect of high pCO<sub>2</sub>, which was explained by increased high-light stress under OA and a reduction in the energy transfer  
efficiency from photochemistry to biomass build-up (Hoppe et al., 2015). In the current study, there was no significant  
interaction between light regime and pCO<sub>2</sub> (p > 0.05, Fig. 2, 3; Table 2, 3). These opposing responses could be caused by  
group- or species-specific differences in carbon acquisition. Diatoms, for example, have highly effective CCMs (Burkhardt  
et al., 2001), which are energetically expensive (Hopkinson et al., 2011). As CCMs allow cells to efficiently sink energy  
360 under sudden high light (Rost et al., 2006), their downregulation in response to high pCO<sub>2</sub> can reduce the ability of cells to  
deal with high-light stress under OA (Hoppe et al., 2015). In contrast to other groups/taxa, which were often found to lose  
their ability to cope with excess energy under OA and dynamic light (e.g. Gao et al., 2012), *M. pusilla* maintained effective  
acclimation without photoinactivation under these conditions. This could be attributed to its size, making it less reliant  
CCMs as a mechanism to reduce reductive pressure under high light, as well as to the observed high plasticity in  
365 photophysiological characteristics under dynamic light (Table 3).

In conclusion, the photoacclimation strategies of *M. pusilla* were optimised for the dynamic light field and did not  
seem to depend on CCMs, therefore the previously observed interaction between pCO<sub>2</sub> and dynamic light (Gao et al., 2012;  
Hoppe et al., 2015; Jin et al., 2013) was not observed here. Thus, the results of this study highlight that it is crucial to  
investigate and understand the underlying physiological mechanisms of observed multi-driver responses in order to judge  
370 whether generalizations from individual studies are feasible or not.



#### 4.4 Implications for the future Arctic Ocean

375 The findings of this study highlight the importance of considering a dynamic light field in laboratory studies, as numerous  
parameters including growth rates were significantly altered when compared to constant irradiance. The common use of  
constant light fields may substantially underestimate the energetic costs of photoacclimation under in-situ conditions (Köhler  
et al., 2018). Therefore, dynamic light fields need to be included when predicting future ecosystem functioning. If the  
responses of the strain used in this study are representative for this species, *M. pusilla* can be expected to cope well with  
380 dynamic light field typical for the surface mixed layer (Table 2, 3). While phytoplankton were often found to suffer from OA  
under dynamic light (Gao et al., 2012; Hoppe et al., 2015; Jin et al., 2013), *M. pusilla* benefitted slightly from OA  
irrespective of the light treatment applied. As beneficial effects by OA were also evident under different temperatures  
(Hoppe et al., 2018), we can conclude that *M. pusilla* has a high plasticity toward OA, warming and difference in light  
regimes, making it well-adapted for conditions expected for the future Arctic ocean. The high physiological plasticity may  
385 thus also explain why picoeukaryotes are often found to dominate mesocosm assemblages under OA (Brussaard et al., 2013;  
Engel et al., 2008; Schulz et al., 2017).

Global warming is, due to the phenomenon of Arctic Amplification (Screen and Simmonds, 2010), a particularly  
important driver for Arctic phytoplankton. *M. pusilla* has been shown to synergistically benefit from OA and warming  
(Hoppe et al., 2018), but future studies should investigate whether responses differ under dynamic light. Furthermore,  
390 warming causes ocean freshening (Peterson et al., 2002) and enhanced stratification, that further reduces nutrient availability  
(Steinacher et al., 2010). Picoeukaryotes may also benefit from these anticipated changes in nutrient supply due to their high  
surface : volume ratio allowing effective nutrient uptake (Li et al., 2009). Changes in the community size structure are  
biogeochemically important as picoplankton-dominated systems tend to be less efficient with respect to carbon export to  
depth (Worden et al., 2015). If smaller phytoplankton become more dominant the Arctic pelagic food web, this may benefit  
395 smaller grazers. With this additional steps in the food web, energy transfer efficiency to top-predators as well as into the  
deep ocean will decrease (Brussaard et al., 2013). Based on the current study, increased abundances of *M. pusilla* under  
future  $p\text{CO}_2$  levels can be expected not only for the more stable low light environments, but also for the productive mixed  
layer in spring-time with its dynamic light fields.

#### 400 Author contributions

CJMH designed and supervised the study. EW conducted the research and wrote the paper with contributions from CJMH  
and BR.

#### Competing interest

405 The authors declare that they have no conflict of interest.

#### Acknowledgements

We are grateful for field support by the 2014/15 station team of the AWIPEV base in Ny-Ålesund (Svalbard) as well as K.  
Wolf's help with strain isolation and maintenance of *M. pusilla* cultures. L. Wischniewski, C. Schallenberg, T. Brenneis and  
410 M. Machnik are acknowledged for assistance in the laboratory.



415

## References

- AMAP: AMAP Assessment 2018: Arctic Ocean Acidification. Arctic Monitoring and Assessment Programme (AMAP), Tromsø, Norway, 187, 2018.
- 420 Apel, K., and Hirt, H.: Reactive oxygen species: metabolism, oxidative stress, and signal transduction, *Annu. Rev. Plant Biol.*, 55, 373-399, doi:10.1146/annurev.arplant.55.031903.141701, 2004.
- Arrigo, K. R., van Dijken, G., and Pabi, S.: Impact of a shrinking Arctic ice cover on marine primary production, *Geophys. Res. Lett.*, 35, doi:10.1029/2008GL035028, 2008.
- Asada, K.: The water-water cycle in chloroplasts: Scavenging of Active Oxygens and Dissipation of Excess Photons, *Annu. Rev. Plant Physiol. Plant Mol. Biol.*, 50, 601-639, doi:10.1146/annurev.arplant.50.1.601, 1999.
- 425 Bach, L. T., Mackinder, L. C., Schulz, K. G., Wheeler, G., Schroeder, D. C., Brownlee, C., and Riebesell, U.: Dissecting the impact of CO<sub>2</sub> and pH on the mechanisms of photosynthesis and calcification in the coccolithophore *Emiliania huxleyi*, *New Phytol.*, 199, 121-134, doi:10.1111/nph.12225, 2013.
- Bates, N. R., and Mathis, J. T.: The Arctic Ocean marine carbon cycle: evaluation of air-sea CO<sub>2</sub> exchanges, ocean acidification impacts and potential feedbacks, *Biogeosciences*, 6, 2433-2459, doi:10.5194/bg-6-2433-2009, 2009.
- 430 Behrenfeld, M. J., Prasil, O., Kolber, Z. S., Babin, M., and Falkowski, P. G.: Compensatory changes in photosystem II electron turnover rates protect photosynthesis from photoinhibition, *Photosynth. Res.*, 58, 259-268, doi:10.1023/A:1006138630573, 1998.
- Behrenfeld, M. J., Halsey, K. H., and Milligan, A. J.: Evolved physiological responses of phytoplankton to their integrated growth environment, *Philos. Trans. R. Soc. Lond. B. Biol. Sci.*, 363, 2687-2703, doi:10.1098/rstb.2008.0019, 2008.
- 435 Blankenship, R. E.: *Molecular mechanisms of photosynthesis*, 2nd Edn, Wiley Blackwell, USA, 2014.
- Brading, P., Warner, M. E., Davey, P., Smith, D. J., Achterberg, E. P., and Suggett, D. J.: Differential effects of ocean acidification on growth and photosynthesis among phylotypes of *Symbiodinium* (Dinophyceae), *Limnol. Oceanogr.*, 56, 927-938, doi:10.4319/lo.2011.56.3.0927, 2011.
- 440 Brewer, P. G., Bradshaw, A., and Williams, R.: Measurements of total carbon dioxide and alkalinity in the North Atlantic Ocean in 1981, in: *The changing carbon cycle*, Springer, 348-370, doi:10.1007/978-1-4757-1915-4\_18, 1986.
- Brussaard, C. P. D., Noordeloos, A. A. M., Witte, H., Collenteur, M. C. J., Schulz, K., Ludwig, A., and Riebesell, U.: Arctic microbial community dynamics influenced by elevated CO<sub>2</sub> levels, *Biogeosciences*, 10, 719-731, doi:10.5194/bg-10-719-2013, 2013.
- 445 Burkhardt, S., Amoroso, G., Riebesell, U., and Sültemeyer, D.: CO<sub>2</sub> and HCO<sub>3</sub><sup>-</sup> uptake in marine diatoms acclimated to different CO<sub>2</sub> concentrations, *Limnol. Oceanogr.*, 46, 1378-1391, doi:10.4319/lo.2001.46.6.1378, 2001.
- Denman, K. L., and Gargett, A. E.: Time and space scales of vertical mixing and advection of phytoplankton in the upper ocean, *Limnol. Oceanogr.*, 28, 801-815, doi:10.4319/lo.1983.28.5.0801, 1983.
- Dickson, A. G., and Millero, F. J.: A comparison of the equilibrium constants for the dissociation of carbonic acid in seawater media, *Deep Sea Res. Part A. Oceanogr. Res. Pap.*, 34, 1733-1743, doi:10.1016/0198-0149(87)90021-5, 1987.
- 450 Dickson, A. G., Sabine, C. L., and Christian, J. R.: *Guide to best practices for ocean CO<sub>2</sub> measurements*, PICES special publications 3, Canada, 2007.
- Engel, A., Schulz, K. G., Riebesell, U., Bellerby, R., Delille, B., and Schartau, M.: Effects of CO<sub>2</sub> on particle size distribution and phytoplankton abundance during a mesocosm bloom experiment (PeECE II), *Biogeosciences*, 5, 509-521, doi:10.5194/bg-5-509-2008, 2008.
- 455



- Falkowski, P. G.: Light-shade adaptation in marine phytoplankton, in: Primary productivity in the sea, vol 19, Springer, Boston, MA, 1980.
- Falkowski, P. G., and Raven, J. A.: Aquatic photosynthesis (Second Edition), Princeton University Press, USA, 2013.
- Fu, F.-X., Warner, M. E., Zhang, Y., Feng, Y., and Hutchins, D. A.: Effects of Increased Temperature and CO<sub>2</sub> on  
460 Photosynthesis, Growth, and Elemental Ratios in Marine Synechococcus and Prochlorococcus (Cyanobacteria), *J. Phycol.*,  
43, 485-496, doi:10.1111/j.1529-8817.2007.00355.x, 2007.
- Gao, K., Helbling, E. W., Häder, D. P., and Hutchins, D. A.: Responses of marine primary producers to interactions between  
ocean acidification, solar radiation, and warming, *Mar. Ecol. Prog. Ser.*, 470, 167-189, doi:10.3354/meps10043, 2012.
- Granskog, M. A., Stedmon, C. A., Dodd, P. A., Amon, R. M. W., Pavlov, A. K., de Steur, L., and Hansen, E.: Characteristics  
465 of colored dissolved organic matter (CDOM) in the Arctic outflow in the Fram Strait: Assessing the changes and fate of  
terrigenous CDOM in the Arctic Ocean, *J. Geophys. Res.: Oceans*, 117, doi:10.1029/2012jc008075, 2012.
- Guillard, R. R., and Ryther, J. H.: Studies of marine planktonic diatoms. I. *Cyclotella nana* Hustedt, and *Detonula  
confervacea* (Cleve) Gran, *Can. J. Microbiol.*, 8, 229-239, doi:10.1139/m62-029, 1962.
- Hopkinson, B. M., Dupont, C. L., Allen, A. E., and Morel, F. M.: Efficiency of the CO<sub>2</sub>-concentrating mechanism of  
470 diatoms, *Proc. Natl. Acad. Sci. USA*, 108, 3830-3837, doi:10.1073/pnas.1018062108, 2011.
- Hoppe, C. J., Holtz, L. M., Trimborn, S., and Rost, B.: Ocean acidification decreases the light-use efficiency in an Antarctic  
diatom under dynamic but not constant light, *New Phytol.*, 207, 159-171, doi:10.1111/nph.13334, 2015.
- Hoppe, C. J., Schuback, N., Semeniuk, D. M., Maldonado, M. T., and Rost, B.: Functional Redundancy Facilitates  
Resilience of Subarctic Phytoplankton Assemblages toward Ocean Acidification and High Irradiance, *Front. Mar. Sci.*, 4,  
475 229, doi:10.3389/fmars.2017.00229, 2017.
- Hoppe, C. J. M., Flintrop, C. M., and Rost, B.: The Arctic picoeukaryote *Micromonas pusilla* benefits synergistically from  
warming and ocean acidification, *Biogeosciences*, 15, 4353-4365, doi:10.5194/bg-15-4353-2018, 2018.
- Houghton, J., Ding, Y., and Griggs, D.: Climate Change: Scientific Basis, IPCC TAR Working Group 1, The Press  
Syndicate of Cambridge University, UK, 2001.
- 480 Huisman, J.: Population dynamics of light-limited phytoplankton: microcosm experiments, *Ecology*, 80, 202-210, doi:  
10.1890/0012-9658(1999)080[0202:PDOLLP]2.0.CO;2, 1999.
- Iglesias-Rodriguez, M., Nimer, N., and Merrett, M.: Carbon dioxide-concentrating mechanism and the development of  
extracellular carbonic anhydrase in the marine picoeukaryote *Micromonas pusilla*, *New Phytol.*, 140, 685-690, doi:  
doi:10.1046/j.1469-8137.1998.00309.x, 1998.
- 485 Jin, P., Gao, K., Villafañe, V. E., Campbell, D. A., and Helbling, W.: Ocean acidification alters the photosynthetic responses  
of a coccolithophorid to fluctuating UV and visible radiation, *Plant Physiol.*, 162, 2084-2094, doi:10.1104/pp.113.219543,  
2013.
- Kim, D., Watanabe, M., Nakayasu, Y., and Kohata, K.: Production of superoxide anion and hydrogen peroxide associated  
with cell growth of *Chattonella antiqua*, *Aquat. Microb. Ecol.*, 35, 57-64, doi:10.3354/ame035057, 2004.
- 490 Kim, J.-H., Kim, K., Kang, E., Lee, K., Kim, J.-M., Park, K.-T., Shin, K., Hyun, B., and Jeong, H.: Enhancement of  
photosynthetic carbon assimilation efficiency by phytoplankton in the future coastal ocean, *Biogeosciences*, 10, 7525-7535,  
doi:10.5194/bg-10-7525-2013, 2013.
- Klughammer, C. and Schreiber, U.: Complementary PS II quantum yields calculated from simple fluorescence parameters  
measured by PAM fluorometry and the Saturation Pulse method. *PAM Appl. Notes* 1, 27-35, 2008.
- 495 Köhler, J., Wang, L., Guislain, A., and Shatwell, T.: Influence of vertical mixing on light-dependency of phytoplankton  
growth, *Limnol. Oceanogr.*, 63, 1156-1167, doi:10.1002/lno.10761, 2018.



- Kolber, Z. S., Prášil, O., and Falkowski, P. G.: Measurements of variable chlorophyll fluorescence using fast repetition rate techniques: defining methodology and experimental protocols, *Biochim. Biophys. Acta. Bioenerg.*, 1367, 88-106, doi: 10.1016/S0005-2728(98)00135-2, 1998.
- 500 Kramer, D.M., Johnson, G., Kiirats, O., Edwards, G. E.: New fluorescence parameters for the determination of QA redox state and excitation energy fluxes, *Photosynth. Res.* 79, 209–218, doi:10.1023/B:PRES.0000015391.99477.0d, 2004.
- Li, W. K., McLaughlin, F. A., Lovejoy, C., and Carmack, E. C.: Smallest algae thrive as the Arctic Ocean freshens, *Science*, 326, 539-539, doi:10.1126/science.1179798, 2009.
- Litchman, E.: Growth rates of phytoplankton under fluctuating light, *Freshwater Biol.*, 44, 223-235, doi:10.1046/j.1365-2427.2000.00559.x, 2000.
- 505 Litchman, E., Klausmeier, C. A., and Bossard, P.: Phytoplankton nutrient competition under dynamic light regimes, *Limnol. Oceanogr.*, 49, 1457-1462, doi:10.4319/lo.2004.49.4\_part\_2.1457, 2004.
- Lohbeck, K. T., Riebesell, U., and Reusch, T. B.: Adaptive evolution of a key phytoplankton species to ocean acidification, *Nat. Geosci.*, 5, 346, doi:10.1038/ngeo1441, 2012.
- 510 Lovejoy, C., Vincent, W. F., Bonilla, S., Roy, S., Martineau, M. J., Terrado, R., Potvin, M., Massana, R., and Pedrós-Alió, C.: Distribution, phylogeny, and growth of cold-adapted picoprasinophytes in Arctic Seas, *J. Phycol.*, 43, 78-89, doi:10.1111/j.1529-8817.2006.00310.x, 2007.
- Maat, D. S., Crawford, K. J., Timmermans, K. R., and Brussaard, C. P.: Elevated pCO<sub>2</sub> and phosphate limitation favor *Micromonas pusilla* through stimulated growth and reduced viral impact, *Appl. Environ. Microbiol.*, 80, 3119-3127, doi:10.1128/AEM.03639-13, 2014.
- 515 MacIntyre, H. L., Kana, T. M., and Geider, R. J.: The effect of water motion on short-term rates of photosynthesis by marine phytoplankton, *Trends Plant Sci.*, 5, 12-17, doi:10.1016/S1360-1385(99)01504-6, 2000.
- Marquardt, M., Vader, A., Stübner, E. I., Reigstad, M. and Gabrielsen, T. M.: Strong seasonality of marine microbial eukaryotes in a high-arctic fjord (Isfjorden, in West Spitsbergen, Norway). *Appl. Environ. Microbiol.*, 82, 1868-1880, doi:10.1128/AEM.03208-15, 2016.
- 520 McKie-Krisberg, Z. M., and Sanders, R. W.: Phagotrophy by the picoeukaryotic green alga *Micromonas*: implications for Arctic Oceans, *ISME J*, 8, 1953-1961, doi:10.1038/ismej.2014.16, 2014.
- Meakin, N. G., and Wyman, M.: Rapid shifts in picoeukaryote community structure in response to ocean acidification, *ISME J.*, 5, 1397-1405, doi:10.1038/ismej.2011.18, 2011.
- 525 Mehrbach, C., Culbertson, C., Hawley, J., and Pytkowicz, R.: Measurement of the apparent dissociation constants of carbonic acid in seawater at atmospheric pressure, *Limnol. Oceanogr.*, 18, 897-907, doi:10.4319/lo.1973.18.6.0897, 1973.
- Miller, G. H., Alley, R. B., Brigham-Grette, J., Fitzpatrick, J. J., Polyak, L., Serreze, M. C., and White, J. W.: Arctic amplification: can the past constrain the future?, *Quat. Sci. Rev.*, 29, 1779-1790, doi:10.1016/j.quascirev.2010.02.008, 2010.
- Mills, M. M., Kropuenske, L. R., Van Dijken, G. L., Alderkamp, A. C., Berg, G. M., Robinson, D. H., Welschmeyer, N. A., and Arrigo, K. R.: Photophysiology in two southern ocean phytoplankton taxa: Photosynthesis of *Phaeocystis* Antarctica (prymnesiophyceae) and *Fragilariopsis cylindrus* (bacillariophyceae) under simulated mixed-layer irradiance, *J. Phycol.*, 46, 1114-1127, doi:10.1111/j.1529-8817.2010.00923.x, 2010.
- 530 Newbold, L. K., Oliver, A. E., Booth, T., Tiwari, B., Desantis, T., Maguire, M., Andersen, G., van der Gast, C. J., and Whiteley, A. S.: The response of marine picoplankton to ocean acidification, *Environ. Microbiol.*, 14, 2293-2307, doi:10.1111/j.1462-2920.2012.02762.x, 2012.
- 535 Nöthig, E.-M., Bracher, A., Engel, A., Metfies, K., Niehoff, B., Peeken, I., Bauerfeind, E., Cherkasheva, A., Gäbler-Schwarz, S., and Hardge, K.: Summertime plankton ecology in Fram Strait—a compilation of long-and short-term observations, *Polar Res.*, 34, 23349, doi:10.3402/polar.v34.23349, 2015.



- Oxborough, K., Baker, N. R., Resolving chlorophyll a fluorescence images of photosynthetic efficiency into photochemical and non-photochemical components – calculation of  $qP$  and  $Fv'/Fm'$ ; without measuring  $Fo'$ , *Photosynth. Res.* 54, 135–142, doi:10.1023/A:1005936823310, 1997.
- Oxborough, K., Moore, C. M., Suggett, D. J., Lawson, T., Chan, H. G., and Geider, R. J.: Direct estimation of functional PSII reaction center concentration and PSII electron flux on a volume basis: a new approach to the analysis of Fast Repetition Rate fluorometry (FRRf) data, *Limnol. Oceanogr.* 10, 142–154, doi: 10.4319/lom.2012.10.142, 2012.
- Pachauri, R. K., Allen, M. R., Barros, V. R., Broome, J., Cramer, W., Christ, R., Church, J. A., Clarke, L., Dahe, Q., and Dasgupta, P.: Climate change 2014: synthesis report. Contribution of Working Groups I, II and III to the fifth assessment report of the Intergovernmental Panel on Climate Change, IPCC, Geneva, Switzerland, 2014.
- Palmer, M. A., Van Dijken, G. L., Mitchell, B. G., Seegers, B. J., Lowry, K. E., Mills, M. M., and Arrigo, K. R.: Light and nutrient control of photosynthesis in natural phytoplankton populations from the Chukchi and Beaufort seas, Arctic Ocean, *Limnol. Oceanogr.*, 58, 2185–2205, doi:10.4319/lo.2013.58.6.2185, 2013.
- Peterson, B. J., Holmes, R. M., McClelland, J. W., Vorosmarty, C. J., Lammers, R. B., Shiklomanov, A. I., Shiklomanov, I. A., and Rahmstorf, S.: Increasing river discharge to the Arctic Ocean, *Science*, 298, 2171–2173, doi:10.1126/science.1077445, 2002.
- Pierrot, D., Lewis, E., and Wallace, D.: MS Excel program developed for CO<sub>2</sub> system calculations, ORNL/CDIAC-105a. Carbon Dioxide Information Analysis Center, Oak Ridge National Laboratory, US Department of Energy, Oak Ridge, Tennessee, 2006.
- Pörtner, H.-O., Karl, D. M., Boyd, P. W., Cheung, W., Lluich-Cota, S. E., Nojiri, Y., Schmidt, D. N., Zavialov, P. O., Alheit, J., and Aristegui, J.: Ocean systems, in: Climate change 2014: impacts, adaptation, and vulnerability. Part A: global and sectoral aspects. contribution of working group II to the fifth assessment report of the intergovernmental panel on climate change, C. Field, V. Barros, D. Dokken, K. Mach, M. Mastrandrea, T. Bilir, M. Chatterjee, K. Ebi, Y. Estrada, R. Genova, B. Girma, E. Kissel, A. Levy, S. MacCracken, P. Mastrandrea and L. White (editors), Cambridge University Press, 411–484, Cambridge, UK and NY, USA, 2014.
- Prado, R., Rioboo, C., Herrero, C., Suarez-Bregua, P., and Cid, A.: Flow cytometric analysis to evaluate physiological alterations in herbicide-exposed *Chlamydomonas moewusii* cells, *Ecotoxicology*, 21, 409–420, doi:10.1007/s10646-011-0801-3, 2012.
- Ragni, M., Airs, R. L., Leonardos, N., and Geider, R. J.: Photoinhibition of Psii in *Emiliana Huxleyi* (Haptophyta) under High Light Stress: The Roles of Photoacclimation, Photoprotection, and Photorepair(1), *J. Phycol.*, 44, 670–683, doi:10.1111/j.1529-8817.2008.00524.x, 2008.
- Reinfelder, J. R.: Carbon concentrating mechanisms in eukaryotic marine phytoplankton, *Ann. Rev. Mar. Sci.*, 3, 291–315, doi:10.1146/annurev-marine-120709-142720, 2010.
- Riebesell, U. and Gattuso, J.-P.: Lessons learned from ocean acidification research, *Nat. Clim. Change*, 5, 12–14, 2015.
- Riebesell, U., and Tortell, P. D.: Effects of ocean acidification on pelagic organisms and ecosystems, *Ocean acidification*, Oxford University Press, Oxford, UK, 2011.
- Rokitta, S. D., John, U., and Rost, B.: Ocean acidification affects redox-balance and ion-homeostasis in the life-cycle stages of *Emiliana huxleyi*, *PLoS One*, 7, 1–10, e52212, doi:10.1371/journal.pone.0052212, 2012.
- Rost, B., Riebesell, U., and Sültemeyer, D.: Carbon acquisition of marine phytoplankton: effect of photoperiod length, *Limnol. Oceanogr.*, 51, 12–20, doi:10.4319/lo.2006.51.1.0012, 2006.
- Rost, B., Zondervan, I., and Wolf-Gladrow, D.: Sensitivity of phytoplankton to future changes in ocean carbonate chemistry: current knowledge, contradictions and research directions, *Mar. Ecol.-prog. Ser.*, 373, 227–237, doi:10.3354/meps07776, 2008.



- Schaum, E., Rost, B., Millar, A. J., and Collins, S.: Variation in plastic responses of a globally distributed picoplankton species to ocean acidification, *Nat. Clim. Change*, 3, 298–302, doi:10.1038/nclimate1774, 2012.
- Schaum, C. E., and Collins, S.: Plasticity predicts evolution in a marine alga, *Proc. Biol. Sci.*, 281, 20141486, doi:10.1098/rspb.2014.1486, 2014.
- 585 Schuback, N., Hoppe, C. J., Tremblay, J. É., Maldonado, M. T., and Tortell, P. D.: Primary productivity and the coupling of photosynthetic electron transport and carbon fixation in the Arctic Ocean, *Limnol. Oceanogr.*, 62, 898–921, doi:10.1002/lno.10475, 2017.
- Schulz, K. G., Bach, L. T., Bellerby, R. G., Bermúdez, R., Büdenbender, J., Boxhammer, T., Czerny, J., Engel, A., Ludwig, A., and Meyerhöfer, M.: Phytoplankton blooms at increasing levels of atmospheric carbon dioxide: Experimental evidence for negative effects on prymnesiophytes and positive on small picoeukaryotes, *Front. Mar. Sci.*, 4, 64, doi:10.3389/fmars.2017.00064, 2017.
- 590 Screen, J. A., and Simmonds, I.: The central role of diminishing sea ice in recent Arctic temperature amplification, *Nature*, 464, 1334, doi:10.1038/nature09051, 2010.
- Shatwell, T., Nicklisch, A., and Köhler, J.: Temperature and photoperiod effects on phytoplankton growing under simulated mixed layer light fluctuations, *Limnol. Oceanogr.*, 57, 541–553, doi:10.4319/lo.2012.57.2.0541, 2012.
- Steinacher, M., Joos, F., Frölicher, T., Bopp, L., Cadule, P., Cocco, V., Doney, S. C., Gehlen, M., Lindsay, K., and Moore, J. K.: Projected 21st century decrease in marine productivity: a multi-model analysis, *Biogeosciences*, 7, 979–1005, doi:10.5194/bg-7-979-2010, 2010.
- Stoll, M., Bakker, K., Nobbe, G., and Haese, R.: Continuous-flow analysis of dissolved inorganic carbon content in seawater, *Anal. Chem.*, 73, 4111–4116, doi:10.1021/ac010303r, 2001.
- 600 Su, W., Jakob, T., and Wilhelm, C.: The Impact of Nonphotochemical Quenching of Fluorescence on the Photon Balance in Diatoms under Dynamic Light Conditions(1), *J. Phycol.*, 48, 336–346, doi:10.1111/j.1529-8817.2012.01128.x, 2012.
- Suggett, D. J., Le Floc’H, E., Harris, G. N., Leonardos, N., and Geider, R. J.: Different strategies of photoacclimation by two strains of *Emiliania huxleyi* (Haptophyta) *J. Phycol.*, 43, 1209–1222, doi:10.1111/j.1529-8817.2007.00406.x, 2007.
- 605 Suggett, D. J., Prášil, O., and Borowitzka, M. A.: Chlorophyll a fluorescence in aquatic sciences: methods and applications, *Developments in Applied Phycology*, Vol 4, Springer, Netherlands, 2010.
- Talmy, D., Blackford, J., Hardman-Mountford, N. J., Dumbrell, A. J., and Geider, R. J.: An optimality model of photoadaptation in contrasting aquatic light regimes, *Limnol. Oceanogr.*, 58, 1802–1818, doi:10.4319/lo.2013.58.5.1802, 2013.
- 610 Tremblay, J.-É., Anderson, L. G., Matrai, P., Coupel, P., Bélanger, S., Michel, C., and Reigstad, M.: Global and regional drivers of nutrient supply, primary production and CO<sub>2</sub> drawdown in the changing Arctic Ocean, *Prog. Oceanogr.*, 139, 171–196, doi:10.1016/j.pocean.2015.08.009, 2015.
- Trenberth, K., Jones, P., Ambenje, P., Bojariu, R., Easterling, D., Klein Tank, A., Parker, D., Rahimzadeh, F., Renwick, J., and Rusticucci, M.: Observations: surface and atmospheric climate change. Chapter 3, *Climate change*, 235–336, 2007.
- 615 Trimborn, S., Thoms, S., Petrou, K., Kranz, S. A., and Rost, B.: Photophysiological responses of Southern Ocean phytoplankton to changes in CO<sub>2</sub> concentrations: short-term versus acclimation effects, *J. Exp. Mar. Biol. Ecol.*, 451, 44–54, doi:10.1016/j.jembe.2013.11.001, 2014.
- Uppström, L. R.: The boron/chlorinity ratio of deep-sea water from the Pacific Ocean, *Deep-Sea Res. and Oceanogr. Abstr.*, 1974, 21, 161–162, doi:10.1016/0011-7471(74)90074-6
- 620 Van Leeuwe, M., and Stefels, J.: Photosynthetic responses in *Phaeocystis antarctica* towards varying light and iron conditions, in: *Phaeocystis, major link in the biogeochemical cycling of climate-relevant elements*, Springer, 61–70, doi:10.1007/978-1-4020-6214-8\_6, 2007.



- Wagner, H., Jakob, T., and Wilhelm, C.: Balancing the energy flow from captured light to biomass under fluctuating light conditions, *New Phytol.*, 169, 95-108, doi:10.1111/j.1469-8137.2005.01550.x, 2006.
- 625 Wassmann, P., and Reigstad, M.: Future Arctic Ocean seasonal ice zones and implications for pelagic-benthic coupling, *Oceanography*, 24, 220-231, doi:10.5670/oceanog.2011.74, 2011.
- Webb, W. L., Newton, M., and Starr, D.: Carbon dioxide exchange of *Alnus rubra*: A mathematical model, *Oecologia*, 17, 281-291, doi:10.1007/BF00345747, 1974.
- Worden, A. Z., Follows, M. J., Giovannoni, S. J., Wilken, S., Zimmerman, A. E. and Keeling, P. J.: Rethinking the marine carbon cycle: factoring in the multifarious lifestyles of microbes. *Science*, 347, 1257594, doi:10.1126/science.1257594, 2015.
- 630 Xu, K., Grant-Burt, J.L., Donaher, N. and Campbell, D.A.: Connectivity among Photosystem II centers in phytoplankters: Patterns and responses. *Biochim. Biophys. Acta (BBA)-Bioenergetics*, 1858(6), 459-474, doi:10.1016/j.bbabi.2017.03.003, 2017.
- 635
- 640

**Table 1.** Carbonate chemistry measurements, for each light and  $p\text{CO}_2$  treatment, from the start and end of the experiment ( $n=4$ ; mean  $\pm$  one SD). The measured values are  $C_T$  (dissolved inorganic carbon),  $A_T$  (total alkalinity) and pH (NBS scale).  $p\text{CO}_2$  was calculated using the  $\text{CO}_{2\text{SYS}}$  program, with pH and  $A_T$  as input values. The values were calculated for  $2^\circ\text{C}$ , with a salinity of 32.2. The nutrient levels were  $6.5 \mu\text{mol kg}^{-1}$  and  $100 \mu\text{mol kg}^{-1}$  for  $\text{PO}_4$  and  $\text{SiOH}_4$ , respectively.

Light Treatment	$p\text{CO}_2$ [ $\mu\text{atm}$ ]	Time Point	$C_T$ [ $\mu\text{mol kg}^{-1}$ ]	$A_T$ [ $\mu\text{mol kg}^{-1}$ ]	pH NBS scale	$p\text{CO}_2$ [ $\mu\text{atm}$ ]
Constant Light	400	Start	$2105 \pm 28$	$2212 \pm 6$	$8.19 \pm 0.06$	$358 \pm 47$
		End	$2122 \pm 16$	$2194 \pm 8$	$8.15 \pm 0.07$	$397 \pm 64$
	1000	Start	$2159 \pm 14$	$2216 \pm 6$	$7.86 \pm 0.01$	$817 \pm 24$
		End	$2202 \pm 6$	$2215 \pm 5$	$7.79 \pm 0.02$	$956 \pm 49$
Dynamic Light	400	Start	$2134 \pm 9$	$2200 \pm 6$	$8.11 \pm 0.03$	$443 \pm 31$
		End	$2156 \pm 15$	$2207 \pm 8$	$8.05 \pm 0.03$	$510 \pm 37$
	1000	Start	$2205 \pm 17$	$2204 \pm 4$	$7.82 \pm 0.03$	$886 \pm 53$
		End	$2216 \pm 11$	$2208 \pm 7$	$7.79 \pm 0.02$	$963 \pm 53$



**Table 2.** Growth and cellular composition of *M. pusilla* (n=4; mean ± one SD), including the growth rate ( $d^{-1}$ ), the division rate constant ( $k$ ), POC production ( $fmol\ cell^{-1}\ day^{-1}$ ), POC quota ( $fmol\ cell^{-1}$ ), PON quota ( $fmol\ cell^{-1}$ ), Chlorophyll  $a$  quota ( $fg\ cell^{-1}$ ), C:N ratio ( $mol\ mol^{-1}$ ) and POC : Chl  $a$  ( $g\ g^{-1}$ ). Treatments include constant light and dynamic light and the two  $pCO_2$  levels of 400  $\mu atm$  and 1000  $\mu atm$ . The letters indicate significant differences between treatments ( $p<0.05$ ) represented as: (a) light, (b)  $pCO_2$ .

Light	$pCO_2$	Growth rate $k$	Division rate	POC production	POC quota	PON quota	Chl $a$ quota	C:N	POC: Chl $a$
Treatment	[ $\mu atm$ ]	[ $d^{-1}$ ]	constant $\mu$ [ $d^{-1}$ ]	[ $fmol\ cell^{-1}\ day^{-1}$ ]	[ $fmol\ cell^{-1}$ ]	[ $fmol\ cell^{-1}$ ]	[ $fg\ cell^{-1}$ ]	[ $mol\ mol^{-1}$ ]	[ $g\ g^{-1}$ ]
Constant Light	400	$0.70 \pm 0.01$	$1.01 \pm 0.01$	$179 \pm 27$	$177 \pm 26$	$19.2 \pm 2.3$	$11.5 \pm 0.49$	$8.8 \pm 0.9$	$185 \pm 28$
	1000	$0.73 \pm 0.02$	$1.06 \pm 0.03$	$170 \pm 31$	$159 \pm 29$	$21.2 \pm 7.6$	$9.4 \pm 0.39$	$9.1 \pm 2.4$	$203 \pm 36$
Dynamic Light	400	$0.37 \pm 0.01$	$0.53 \pm 0.01$	$81 \pm 17$	$151 \pm 28$	$20.3 \pm 4.6$	$10.4 \pm 0.39$	$7.7 \pm 1.0$	$175 \pm 30$
	1000	$0.41 \pm 0.02$	$0.59 \pm 0.03$	$77 \pm 14$	$132 \pm 26$	$18.5 \pm 5.7$	$9.3 \pm 1.07$	$7.7 \pm 1.5$	$172 \pm 42$
Significance		a, b	a	a			b		



645

650

655

660

665

670

675

680

685

690

695

**Table 3.** FRRF-based photophysiological parameters for *M. pusilla* ( $n=4$ ; mean  $\pm$  one SD). Displayed is the  $F_v/F_m$  (dimensionless), the connectivity between PSII's ( $\rho$ ; [dimensionless]), the absorption cross-section of PSII photochemistry ( $\sigma_{PSII}$ ; [ $\text{Å}^2 \cdot \text{q}^{-1}$ ]), the non-photochemical quenching (NPQ; [dimensionless]), the PSII re-opening rate ( $\tau$ , ms), the maximum photosynthetic rate ( $\text{ETR}_{\text{max}}$ ; [ $\text{mol e}^- (\text{mol RCII})^{-1} \text{s}^{-1}$ ]), the light harvesting efficiency ( $\alpha$ ; [ $\text{mol e}^- \text{m}^2 (\text{mol photons})^{-1}$ ]) and the light saturation constant ( $I_k$ ; [ $\mu\text{mol photons m}^{-2} \text{s}^{-1}$ ]) for both light regimes and  $p\text{CO}_2$  levels. The letters indicate significant differences between treatments ( $p < 0.05$ ) represented as: (a) light, (b)  $p\text{CO}_2$ .

Light	$p\text{CO}_2$	$F_v/F_m$	$\rho$	$\sigma_{PSII}$	NPQ	$\tau$	$\text{rETR}_{\text{max}}$	$I_k$	$\alpha$
Treatment	[ $\mu\text{atm}$ ]	Dimensionless	Dimensionless	[ $\text{Å}^2 \cdot \text{q}^{-1}$ ]	Dimensionless	[ms]	( $\text{mol RCII})^{-1} \text{s}^{-1}$ )	$\text{m}^{-2} \text{s}^{-1}$	( $\text{mol e}^- \text{m}^2 (\text{mol RCII})^{-1}$ )
Constant Light	400	$0.46 \pm 0.01$	$0.33 \pm 0.08$	$5.2 \pm 0.1$	$12.7 \pm 1.8$	$617 \pm 9$	$369 \pm 33$	$61.4 \pm 8.0$	$6.0 \pm 0.4$
	1000	$0.49 \pm 0.03$	$0.31 \pm 0.03$	$5.5 \pm 0.1$	$11.4 \pm 3.0$	$600 \pm 11$	$416 \pm 104$	$101.9 \pm 33.3$	$4.8 \pm 1.1$
Dynamic Light	400	$0.54 \pm 0.00$	$0.40 \pm 0.01$	$6.7 \pm 0.4$	$0.7 \pm 0.0$	$573 \pm 24$	$530 \pm 40$	$60.1 \pm 11.8$	$9.0 \pm 1.1$
	1000	$0.54 \pm 0.01$	$0.42 \pm 0.02$	$6.8 \pm 0.4$	$0.7 \pm 0.0$	$569 \pm 20$	$640 \pm 50$	$84.2 \pm 10.4$	$7.6 \pm 0.6$
Significance		a, b	a	a	a	a	a, b	b	a, b



700

705

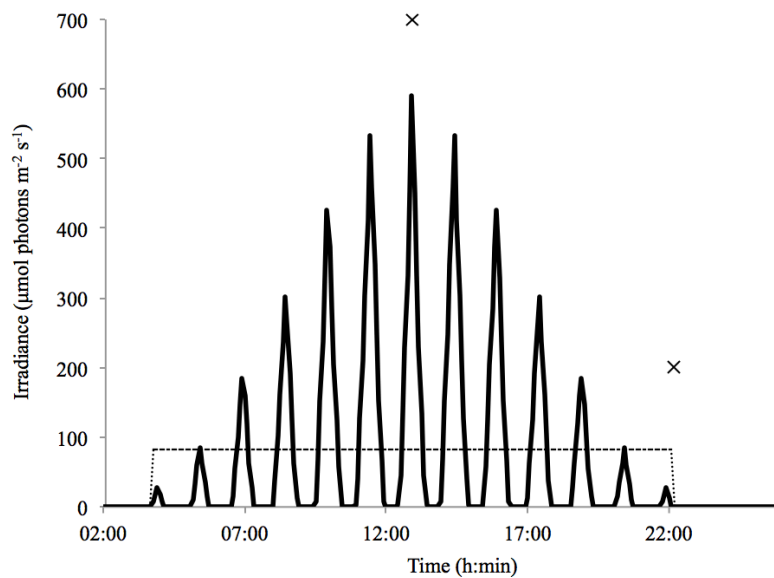
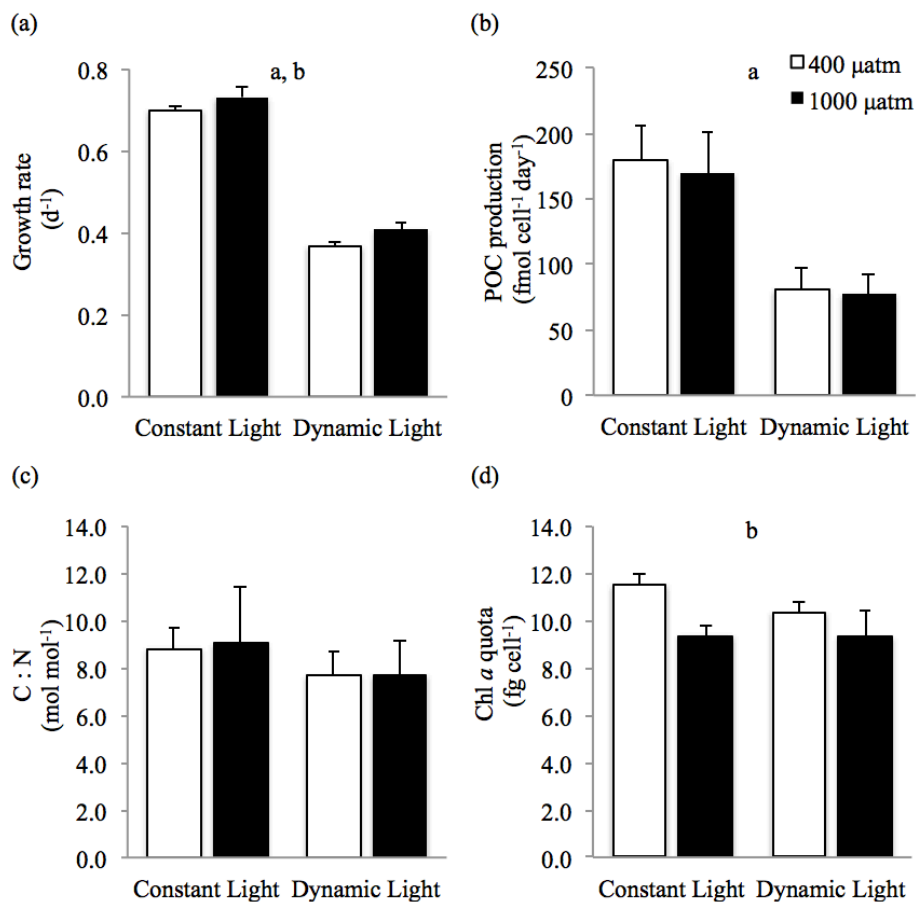


**Figure 1.** Light regimes plotted as a function of time, over a 24 h period. Indicated are the dynamic light cycle (solid line) and the constant light cycle (dashed line). Time point 1 and 2 are displayed at midday, and in the evening at the start of the dark period (x).



710

**Figure 2.** (a) Growth rate (d<sup>-1</sup>), (b) POC production (fmol cell day<sup>-1</sup>), (c) C:N ratio (mol mol<sup>-1</sup>), (d) Chlorophyll *a* quota (fg cell<sup>-1</sup>) of *Micromonas pusilla* under constant light and dynamic light and pCO<sub>2</sub> levels of 400 atm (white) and 1000 atm (black; n=4; mean ± one SD). The letters indicate significant differences between treatments (p < 0.05), represented as: (a) Light (b) pCO<sub>2</sub>

715

720

725

730

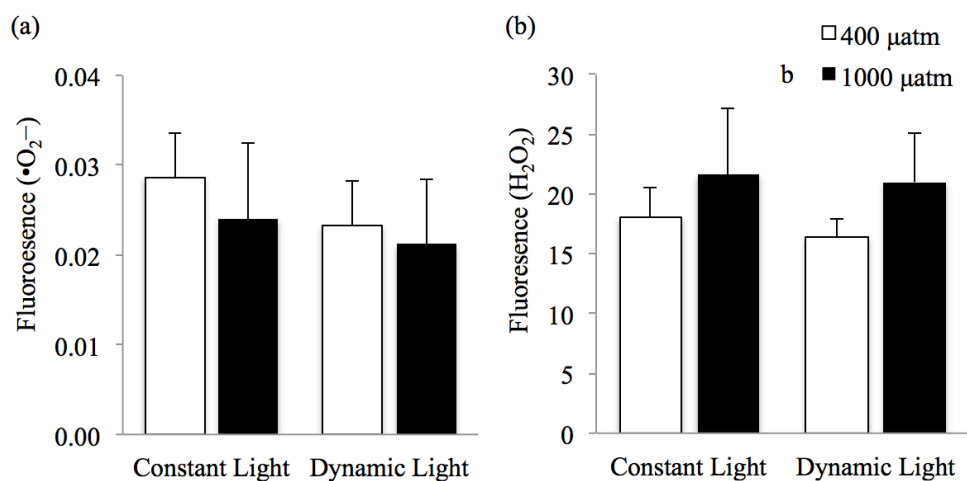


**Figure 3.** The relative production of (a) oxygen free radicals ( $\bullet\text{O}_2^-$ ) and (b) hydrogen peroxide ( $\text{H}_2\text{O}_2$ ) in *Micromonas pusilla* under constant light and dynamic light and  $p\text{CO}_2$  levels of 400  $\mu\text{atm}$  (white) and 1000  $\mu\text{atm}$  (black;  $n=4$ ; mean  $\pm$  one SD) at time point 1. The letters indicate significant differences between treatments ( $p<0.05$ ), represented as: (b)  $p\text{CO}_2$

735

740

745

750